New Solar Physics with Solar-B Mission
ASP Conference Series, Vol. 369, 2007
K. Shibata, S. Nagata, and T. Sakurai

Observational Analysis of the Relation between Coronal Loop Heating and Photospheric Magnetic Fields

Yukio Katsukawa

National Astronomical Observatory, Mitaka, Tokyo 181-8588, Japan

Abstract. The solar corona and the photosphere are linked through magnetic field lines, and heating energy is supposed to be supplied from the footpoints of each coronal loop along magnetic field lines. Thus it is important to examine properties of photospheric magnetic fields at the footpoints of the coronal loops in order to understand heating of the coronal loops. We performed simultaneous observations of photospheric magnetic properties and coronal loop structures using the ground based telescopes and Transition Region And Coronal Explorer (TRACE). Footpoint locations were identified in the TRACE images, and the structure in the photosphere was examined by Advanced Stokes Polarimeter (ASP) or Dutch Open Telescope (DOT). Most of the coronal loops emanating from a sunspot had their footpoints around the boundary between the umbra and the penumbra. Furthermore, bright loops were revealed to have their footpoints at the locations where there was highly interlaced magnetic configuration. We observed fragmentation of an umbra and formation of a light bridge in decaying sunspots, and found possible association between such phenomena in the decaying spots and the coronal loops. These observational results suggest that spatial fluctuation of magnetic fields forms current sheets at the base of the corona, resulting in heating of the coronal loops.

1. Introduction

The energy source for the heating of the corona is magnetic energy generated by interaction between convective motion and magnetic fields in the photosphere. Thus it is important to observe not only the corona, where the magnetic energy is dissipated, but also the photosphere, where the heating energy is generated. The important properties we should consider is that the solar corona is spatially quite non-uniform. Images taken in X-rays and EUV show that the solar corona consists of many loops which are structured by magnetic field lines. Thus it is critically important to clarify what magnetic structure exists at the footpoints of the coronal loops. Furthermore, it becomes clear that individual coronal loops have different temperatures from 1MK to over 5MK. Nagata et al. (2003) clearly showed that hot (over 2MK) loops seen in Yohkoh Soft X-ray Telescope (SXT) images and cool (1MK) loops seen in images taken by Extreme-ultraviolet Imaging Telescope (EIT) are spatially exclusive. In addition, the hot and cool loops are found to have different properties in terms of temperature and density distribution along individual loops (e.g. Kano & Tsuneta 1996; Priest et al. 1998; Aschwanden et al. 2001; Winebarger et al. 2003). These observational results suggest that not only the heating energy but the heating locations are different between the hot and cool loops.

Katsukawa & Tsuneta (2005) investigated differences of photospheric magnetic properties between the hot and cool loops with the Advanced Stokes Polarimeter (ASP). In contrast to the cool loops, the hot loops observed with SXT are usually diffuse, resulting in ambiguous identification of their footpoint locations. They used "moss" structure observed with Transition Region And Coronal Explorer (TRACE), which was confirmed to be low-lying EUV emission at the footpoints of the hot loops. Footpoints of both loops have magnetic fields whose strength is 1.2-1.3 kG, and the orientation is almost vertical to the surface. A significant difference was discovered in the magnetic filling factor, which is defined by the fraction of a pixel filled with a magnetized atmosphere. The footpoints of the hot loops have a lower filling factor than the footpoints of the cool loops. They suggested that braiding of coronal magnetic fields is more efficient at the footpoints of the hot loops than at the footpoints of the cool loops as a result of the combination of the lower filling factor and higher horizontal velocity.

It has been well known that the corona directly above a sunspot is dark in soft X-rays since observations with Skylab and Yohkoh (Vaiana et al. 1976; Vourlidas et al. 1997). These observations indicate that a heating mechanism which is responsible for heating of the hot loops is strongly suppressed in a sunspot. High resolution X-ray and EUV imaging telescopes such as Normal Incidence X-ray Telescope (NIXT), EIT on SOHO, and TRACE have demonstrated that cool loops whose temperatures are 1-2MK are emerging from a sunspot, and form fan-like structure (Sams et al. 1992; Harmon et al. 1993; Schrijver et al. 1999). The temperatures of such loops are not hot enough, so that soft X-ray telescopes such as Yohkoh cannot observe the cool loops.

Although magnetic field lines are supposed to fill the entire volume above a sunspot, only the plasma which is visible in EUV as the coronal loops is heated to around 1 MK, and the temperature of the rest remains below 1 MK. These observational evidence suggests that some heating mechanism might be operated at the positions localized at the footpoints. Sams et al. (1992) found that most of the loops were emerging from the inner penumbra using NIXT, and suggested that complex magnetic structure in the penumbra might be possible cause of the heating. Schrijver et al. (1999) confirmed this tendency by TRACE with exception such as loops emerging from an umbra.

There have been no detailed studies to investigate what magnetic structure exists at the feet of these cool coronal loops. We performed observations of magnetic structures in the photosphere simultaneous with observations of coronae by TRACE. In Section 2 we present the magnetic configuration at the footpoints of the coronal loops revealed with ASP. Fine-scale magnetic signatures located at the footpoints are studied with high resolutional imaging observations by Dutch Open Telescope (DOT) simultaneous with TRACE, and are presented in Section 3. We here concentrate on the coronal loops inside sunspots because we think the corona above a sunspot is ideal site to investigate the formation mechanisms of the cool 1 – 2 MK coronal loops. The loops have a relatively simple structure there, and accurate identification of footpoint locations is easier. Since there is little hot (> 2 MK) coronal plasma there, we may be able to isolate magnetic features responsible for the heating of the cool loops.

Table 1. Footpoint locations in terms of the continuum intensity

	All loops	$I_l > 4$ DN $s^{-1}pix^{-1}$
Total	47	24
Umbra	11 (25%)	8 (33%)
U-P boundary	22 (47%)	12 (50%)
Penumbra	13 (28%)	4 (17%)

2. Interlaced Magnetic Structure at the Footpoints of Coronal Loops

Active region studied here is NOAA 306 observed from Mar 11 to 13, 2003. The region showed a relatively simple magnetic configuration with a large leading spot, and was located near the center of the solar disk during the observing period. There were many coronal loops emanating from the southern and western side of the leading spot, and formed a fan-like structure in TRACE Fe IX/X 171 Å images.

2.1. Footpoint Positions and their Magnetic Properties

It is essential to determine footpoint locations of the coronal loops precisely and systematically for identifying what magnetic structure are connected to the coronal loops. The Fe IX/X 171 Å images obtained with TRACE are processed with the Laplacian filter to enhance the coronal loop structure. We then identify and extract the coronal loops in the filtered images, and make intensity distribution along each loop by averaging 3 pixels (corresponding to 1.5 arcsec) perpendicular to the loops. The intensities increase along each loop from the footpoints, and then reach a peak with around 10 arcsec. We calculate 2nd derivatives for the intensity profiles as a function of distance along each loop. We here define the loop footpoint as the position where the 2nd derivative is equal to 0. The ambiguity in the identification of the footpoints is a few pixels in the TRACE images. The intensity of each loop is defined as the intensity averaged over 20 pixels (corresponding to 10 arcsec) along the loop from its footpoint. We extract 11, 16, and 20 loops from the TRACE images on March 11, 12, and 13, respectively. The loops and their footpoints thus identified are shown in Figure 1. Many footpoints are located near the interface between the umbra and the penumbra.

Magnetic parameters obtained with ASP are investigated for each loop footpoint. Here the magnetic parameters are derived from observed Stokes profiles using the HAO Stokes inversion based on Milne-Eddington least squares fitting. Figure 2 shows a histogram of continuum intensities in the entire region that ASP observed on 12 Mar 2003. There are 3 peaks corresponding to the umbra, the penumbra, and the *quiet* Sun. There is a large intensity gap between the umbra and the penumbra. We here define the umbra-penumbra (U-P) boundary as the region where the continuum intensity I_c is between 0.2 and 0.7 of the quiet Sun intensity as showing in Figure 2.

Table 1 shows the footpoint locations in terms of the continuum intensity. About a half of the loop footpoints are in the U-P boundary region. One third of the loops have their feet in the penumbra. The table also shows the

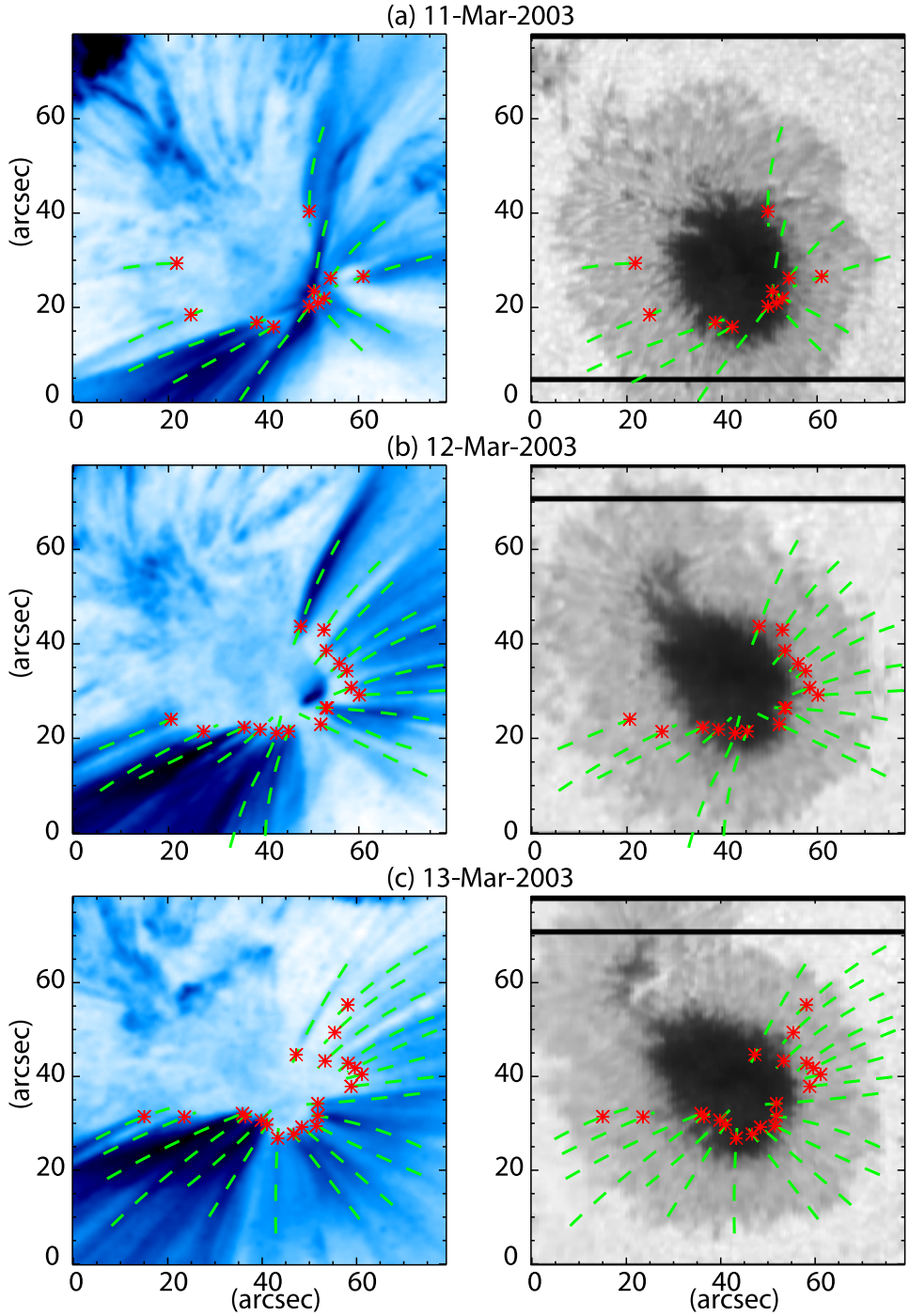

Figure 1. Spatial distribution of the coronal loops observed with TRACE on 11 – 13 Mar 2003. The TRACE Fe IX/X 171 Å images (left) and the continuum images obtained with ASP (right) are shown. The dashed curves indicate the identified loops, and the asterisks indicate the positions of the footpoints.

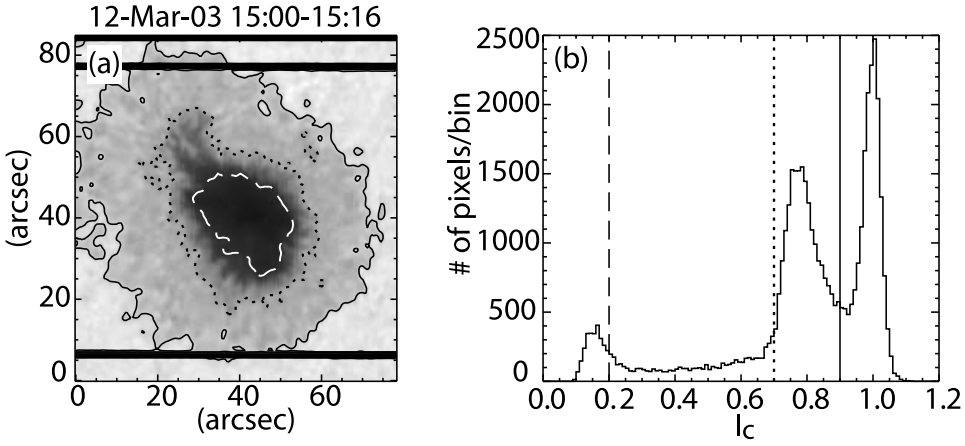

Figure 2. (a) Continuum image on 12 Mar 2003 observed with ASP and (b) the histogram of continuum intensities I_c. The dashed line in the continuum image (a) shows the contours at the intensity $I_c = 0.2$, the dotted line at $I_c = 0.7$, and the solid line at $I_c = 0.9$.

footpoint locations only for the bright loops whose intensity is greater than 4 DN $\sec^{-1}$pixel^{-1}. Over 80 % of the bright loops have footpoints in the umbra and the U-P boundary, and the loops whose footpoints are in the penumbra are found to be faint. This tendency is also recognized in the spatial distribution of the footpoints on the continuum maps shown in Figure 1. Sams et al. (1992) found that loops observed with NIXT were emerging from the inner penumbra, and no loops originated from the umbra. The footpoints of the TRACE loops are here found to be rooted in the umbra and the U-P boundary region rather than the penumbra with the systematic determination of the footpoint locations. Schrijver et al. (1999) also showed that some loops observed with TRACE appeared to terminate in the interface between umbrae and penumbrae.

2.2. Magnetic Structure at the Footpoints

We have shown that most of the coronal loops seen in TRACE 171 Å images have footpoints in the umbra and the U-P boundary. Magnetic parameters have monotonic correlation with the continuum intensity in the U-P boundary region where $0.2 < I_c < 0.7$. As the continuum intensity increases from 0.2 to 0.7, the inclination increases from about 30 deg to 50 deg, the magnetic field strength decreases from about 2.3 kG to 1.3 kG. Such correlation and anti-correlation among the continuum intensity, the magnetic field strength, and the inclination are reported by many authors (e.g. Lites et al. 1993; Stanchfield et al. 1997; Westendorp Plaza et al. 2001).

We examine azimuthal structure of magnetic fields around the U-P boundary region. The contours of $I_c = 0.3$ are created from the ASP continuum intensity maps smoothed with a boxcar average of 5.6 arcsec windows, and are drawn on the continuum map in Figure 3. Along the contours, variation of the photospheric quantities obtained with ASP are plotted as a function of position angle in Figure 3. Here plotted the continuum intensity, the magnetic field strength,

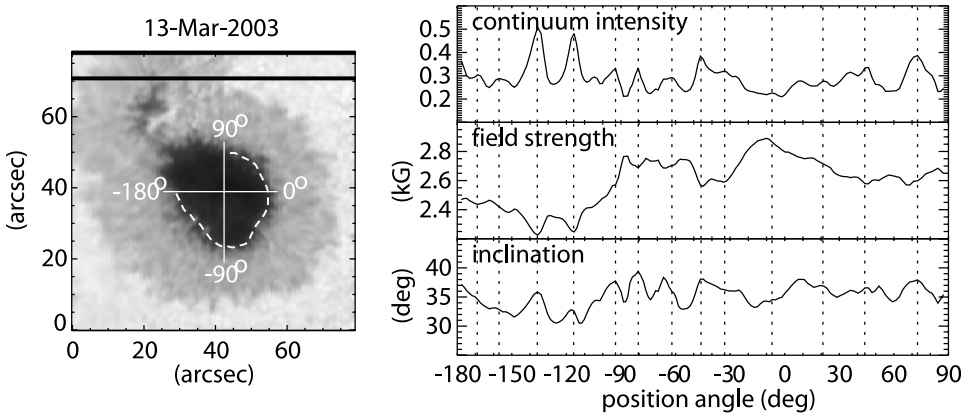

Figure 3. Azimuthal variation of the continuum intensity, the magnetic field strength, and the magnetic inclination along the contour of $I_c = 0.3$, which is drawn by the dashed curve on the continuum map, as a function of azimuthal position angle around the umbra. The position angle is measured counterclockwise from the solar west. The dotted vertical lines locate the local maxima in the continuum intensity.

and the magnetic inclination. Along the contours of $I_c = 0.3$, the continuum intensities are found to fluctuate with an amplitude of about 0.1. Spatial scale of the intensity variation is about 5 arcsec corresponding to about 3600km. The magnetic field strength and inclination also fluctuate simultaneously with the continuum intensity. The local maxima of the continuum intensity are well coincident with the local minima of the field strength, and the local maxima of the inclination. The field strength is about 150G weaker at the local maxima of the continuum intensity, and the inclination is about 5 deg more vertical. The most significant corrugated structure is seen between -140 deg and -110 deg in the position angle for these 3 days. In the U-P boundary region, the dark points in the continuum intensity have umbral magnetic fields, which are strong and vertical, and the bright points have penumbral fields, which are relatively weak and inclined.

It has been known that presence of the azimuthally narrow spines of enhanced magnetic fields which are more vertical than their surroundings (Degenhardt et al. 1991; Title et al. 1993; Lites et al. 1993) in an outer penumbra. Such comb-like interlaced structure (sometimes called fluted structure) is prominent in the outer penumbra, and is not recognized in the umbra. We point out that similar interlaced structure is also visible even in the boundary region as shown in this paper.

We calculate peak-to-valley (P-V) values of the continuum intensities within an interval of 15 deg in the azimuthal position angle along the contours of $I_c = 0.3$ to quantify the magnitude of the corrugation of the magnetic fields in the U-P boundary region. Figure 4 shows the P-V values of the continuum intensities as a function of the azimuthal position angle. The distribution is well representing the significant features visible in the continuum intensity map. Large intensity fluctuation is seen at around the position angle of 120 deg, and

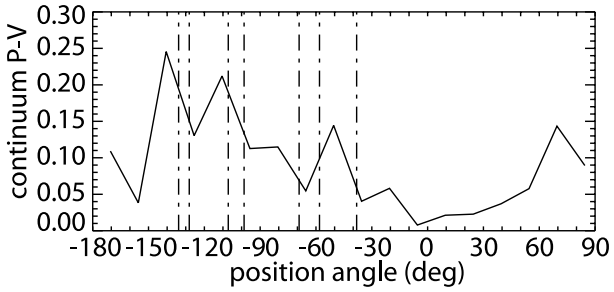

Figure 4. Spatial fluctuation of the continuum intensities along the contour of $I_c = 0.3$ as a function of the azimuthal position angle. The vertical dash-dotted lines indicate the positions of the footpoints for the bright and non-penumbral loops.

this is also recognized in the continuum intensity map shown in Figure 3. The vertical dash-dotted lines in Figure 4 locate the footpoint positions of the loops which have the intensities greater than 4 DN $\sec^{-1}$pixel^{-1} and are not located in the penumbra. The bright loops have two preferred locations in the azimuthal positions for these 3 days. One is from -140 deg to -100 deg in the azimuthal position angle, and the other is from -70 deg to -30 deg. Figure 4 shows that these two preferred regions are clearly coincident with the regions where the enhanced intensity fluctuation is observed.

2.3. Heating of the Coronal Loops in the U-P Boundary Region

Two kinds of magnetic fields are interlaced with the horizontal spatial scale of 3000 – 4000 km in the U-P boundary region. The umbral magnetic fields, which are strong and vertical, and the penumbral fields, which are relatively weak and inclined, may form tangential discontinuities and current sheets between them. We found that the majority of the coronal loops seen in the TRACE 171 Å images have footpoints in the U-P boundary region, and that the footpoints of the bright loops are associated with the interlaced magnetic structure where larger spatial variation is observed in the continuum intensity.

Figure 5 shows a schematic figure of the magnetic structure in the U-P boundary region. A tangential discontinuity between the vertical umbral fields and the inclined penumbral ones has a possibility to dissipate its magnetic energy through magnetic reconnection resulting in heating of the base of the coronal loops. It is often observed that bright penumbral features are moving inward from penumbrae to umbrae with a speed of around 0.4 km s^{-1} (Muller 1973; Kitai 1986; Lites et al. 1998). Such photospheric plasma motion may push the built-in discontinuity to make the current sheet thinner in the corona. This is the condition for the forced magnetic reconnection at the base of the corona. Flat temperature profiles along the cool coronal loops indicate that the heating source is located near the base of the loops (e.g. Aschwanden et al. 2001; Winebarger et al. 2003). The model proposed here is consistent with the concentration of the heating near the loop footpoints.

The magnetic fields in the umbra is nearly vertical to the surface, and spatial variation of magnetic fields is small, so that there is less possibility to

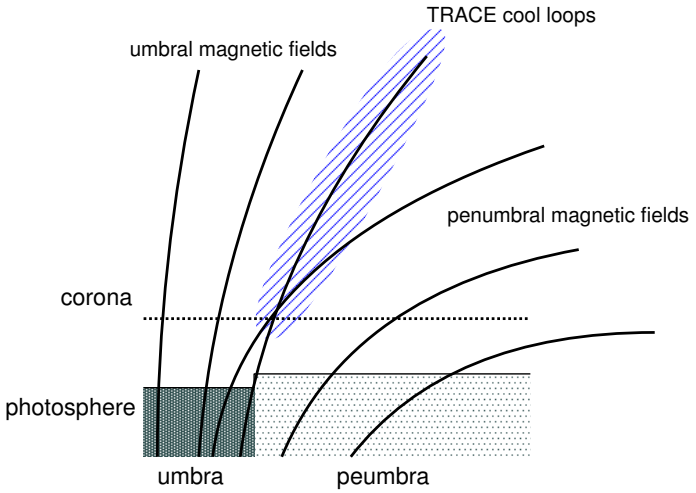

Figure 5. Schematic illustration of magnetic configuration around a sunspot umbra.

have similar built-in current sheet structure. Furthermore, mobilities of magnetic fields is apparently suppressed presumably due to the large field strength. Thus the umbral fields would be unable to generate the heating energy, resulting in dark coronae above umbrae. On the other hand, outer penumbrae provide preferable environment for magnetic reconnection; two essential ingredients of the interlaced magnetic structure and the photospheric velocity fields are both available in the regions. The fields are however nearly parallel to the surface, and would not be able to become coronal loops.

3. Coronal Loops above Decaying Sunspots

We performed a campaign observation in July 2005 using the international time program (ITP) of the telescopes located at Canary islands, Spain. Swedish Solar Telescope (SST) and Dutch Open Telescope (DOT) at La Palma were dedicated to carry out high resolutional imaging observation of the photosphere and the chromosphere. Vacuum Tower Telescope (VTT) at Tenerife was used to perform spectro-polarimetric observations of the photosphere and the chromosphere with Tenerife Infrared Polarimeter (TIP-2) and Polarimetric Littrow Spectrograph (POLIS). The same target region were also observed by SOHO and TRACE to get coronal structures and evolution as Joint Observation Program (JOP) 181. Results obtained by this campaign observation are reported by Shimizu et al. (2006) in this volume. Here we concentrate on the relation between fine photospheric structures and the footpoints location of the coronal loops observed with TRACE. Especially heating of coronal loops in decaying spots are examined here.

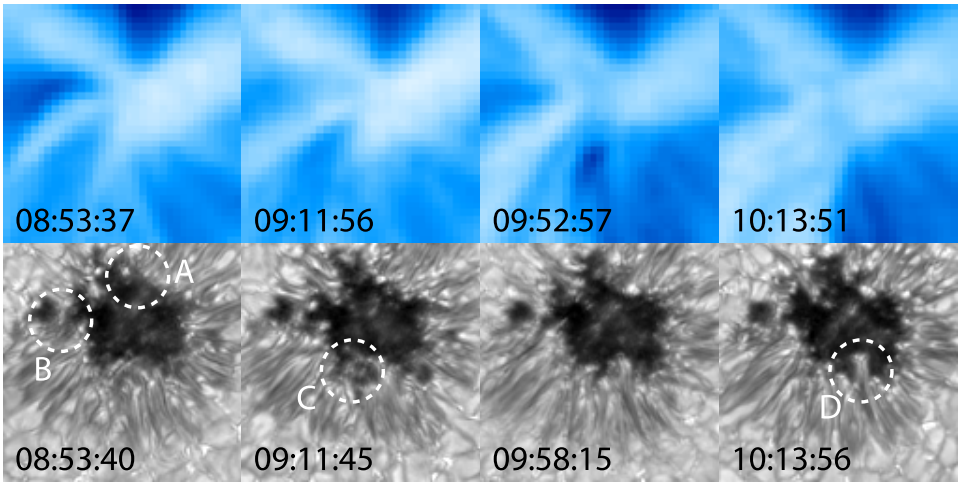

Figure 6. Time evolution of the leading spot in AR 781 from 8 UT to 11 UT on 3 July 2005. Here shown are G-band images observed with DOT (bottom) and Fe IX/X 171 Å images observed with TRACE (top). The FOV size is 18" × 18".

3.1. Fine Photospheric Structure at the Footpoints

A leading spot of the active region NOAA AR 781 was observed on 3 July 2005 by DOT and TRACE. Figure 6 shows time evolution of the spot observed for 1.5 hours. The TRACE 171 Å images are co-aligned with the DOT G-band images using the white light (WL) images taken by TRACE. The diameter of the spot is less than 20 arcsec, and is gradually decreasing from day to day. We can see small dark fragments stripped off from the umbra in the DOT G-band images. Such small fragments are difficult to be recognized in the TRACE WL images because of lower spatial resolution.

The TRACE 171 Å images show that many coronal loops are rooted around the boundary between the umbra and the penumbra. Furthermore the footpoints of the loops seem to have preferred locations as suggested in the previous section. There are persistent loops rooted on the northern side of the umbra for this 1.5 hours. The dashed circle 'A' represent the coarse footpoint locations for the northern loops. One fragment of the umbra is seen in the G-band image at 10:13 UT around the region 'A', but the relation to the persistent heating is not so clear. There is the largest fragment of the umbra in region 'B' for this 1.5 hours, and the bright coronal loops are seen in the first half of the period. Similarly a large fragment is there in region 'C' at 9:11 UT, and we can see a bright loop is transiently heated at 9:52 UT. There is no large fragment of the umbra in region 'D', but many coronal loops are emerging from the region to the southwestern direction. One interesting feature is that a penumbral filament starts to enter into the umbra from 9:58 UT, and the penumbral intrusion is clearly visible in the image at 10:13 UT.

This observational result suggests that fragmentation of the umbra and penumbral intrusion are possible causes of the heating in the decaying spot although the relationship is not confident enough only from this observation.

We have to do statistical analysis in order to clarify the relationship between such fine photospheric features and the loop heating.

3.2. Formation of a Light-bridge and the Loop Heating

A following spot of the AR 789 was continuously observed by TRACE from July 11 to 13. The diameter of the spot is about 30 arcsec on July 11, and is gradually decaying during the observing period. Figure 7 (left) shows time evolution of the spot from July 11 to 12 observed with the TRACE WL band. One clear signature of the decaying process was the formation of a light bridge. The light bridge starts its formation from the western side of the spot at around 6 UT on 11 July. And the formation is completed at around 18 UT on 11 July. The northern portion of the spot is separated from the main spot by the light bridge.

Figure 7 (right) shows time evolution of the corona above the spot observed with TRACE Fe IX/X 171 Å. It is obvious that many coronal loops are rooted in the northern part of the spot for the period, especially near the light bridge. The spot is not completely divided by the light bridge in the initial phase of the formation of the light bridge, and the light bridge is seen only in the western side of the spot. During that period, the coronal loops are bright in the western side of the spot. As the light bridge is developed from the west to the east, the footpoints of the coronal loops move from the west to the east simultaneously, and it is obvious that the footpoints of the loops are associated with the formation of the light bridge. Just after the formation of the light bridge is completed, many coronal loops are emerging from the light bridge, and form a fan-like structure on the northern side of the light bridge. Then the coronae become dark just above the light bridge on 12 July, and the coronal loops are mainly seen around the northern side of the small spot separated by the light bridge. This observational result strongly indicates that the coronal loop heating is related to the magnetic configuration in the light bridge.

The association between some coronal loops observed with TRACE and light bridges was already reported by Schrijver et al. (1999) although detailed studies have not been done yet. Leka (1997) studied vector magnetic fields in light bridges using ASP, and found that there were relatively weak and inclined fields in the light bridges close vertical umbral fields. Jurcak et al. (2006) obtained magnetic configuration of some light bridges with a high resolutional spectro-polarimeter aboard the Swedish Vacuum Solar Telescope (SVST) at La Palma. They analyzed Stokes profiles inside the light bridges with Stokes Inversion based on Response function (SIR), and obtained height dependence of magnetic fields there. They suggested that a canopy-like structure existed above the light bridges. There might be a possibility that strong magnetic discontinuities are created by the canopy fields above the light bridges resulting in the heating of the coronal loops.

4. Summary and Discussion

We investigated the magnetic configuration in the sunspots located at the footpoints of the coronal loops observed with TRACE. In Section 2, we find the interlaced magnetic structure coincides in position with the footpoints of the

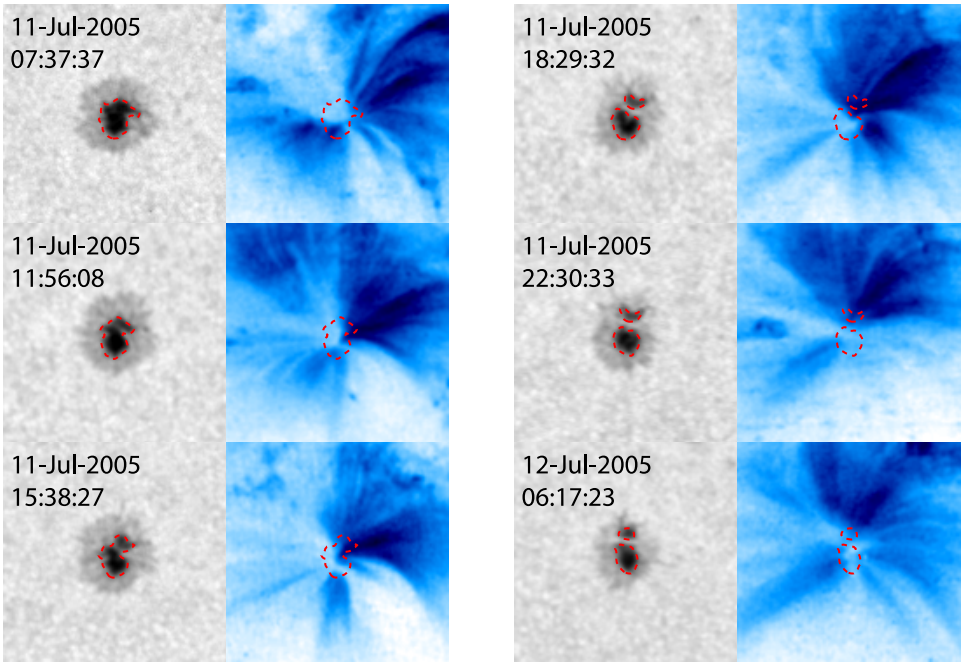

Figure 7. Time evolution of the following spot in AR 789 from 11 July 7 UT to 12 July 6 UT. Here shown are TRACE WL images (left) and Fe IX/X 171 Å images (right). The FOV size is 64" × 64".

loops in the boundary region between the umbra and the penumbra. We show in Section 3 that some coronal loops are possibly associated with fragments of the umbra and the intrusion of the penumbral filament in the decaying spot using the high resolutional observation of the photosphere. The formation of the light bridge is revealed to be coincident with the coronal loops spatially and temporally as shown in Section 3.

Sunspots have strong magnetic fields, but not all the magnetic energies are available to heat the corona. There should be enough photospheric motion in order to braid magnetic field lines and generate magnetic energies available for the heating. Velocities of umbral dots are studied by several authors (e.g. Sobotka et al. 1997), and they showed the velocities are around 0.2 km/s. It has not become clear that such photospheric motion generate enough energies to heat the corona. The observational results presented in this paper suggest that heating of the coronal loops is caused by spatial fluctuation of magnetic fields seen around the boundary between the umbra and the penumbra. Tangential discontinuities or current sheets might be responsible for the heating at the base of the corona. Because the field strength is large in sunspots, not only anti-parallel fields but magnetic fields with small contact angles might be able to generate enough energy.

Observational evidence is still not enough to support this heating scenario. Statistical studies are necessary for many footpoints of coronal loops. Continuous and high resolutional observations by Solar-B may provide an opportunity to

perform such studies. It is also important to measure the magnetic configuration directly in the chromosphere and the transition region.

Acknowledgments. I would like to thank T. Shimizu, R. Kano, V. Martinez Pillet, J. A. Bonet, P. Sütterlin, and S. Tsuneta for fruitful discussion and supporting the campaign observation. I am grateful to T. Tarbell for arranging the coordination of the TRACE observations.

References

Aschwanden, M. J., Schrijver, C. J., & Alexander, D. 2001, ApJ, 550, 1036
Degenhardt, D. & Wiehr, E. 1991, A&A, 252, 821
Harmon, R., Rosner, R., Zirin, H., Spiller, E., & Golub, L. 1993, ApJ, 417, L83
Jurcak, J., Martinez Pillet, V., & Sobotka, M. 2006, A&A, in press
Katsukawa, Y., & Tsuneta, S. 2005, ApJ, 621, 498
Kano, R. & Tsuneta, S. 1996, PASJ, 48, 535
Kitai, R. 1986, Solar Phys., 104, 287
Leka, K. D. 1997, ApJ, 484, 90
Lites, B. W., Elmore, D. F., Seagraves, P., & Skumanich, A. P. 1993,
Lites, B. W., Thomas, J. H., Bogdan, T. J., & Cally, P. S. 1998, ApJ, 497, 464
Muller, R. 1973, Solar Phys., 29, 55
Nagata, S. et al. 2003, ApJ, 590, 1095
Priest, E. R., Foley, C. R., Heyvaerts, J., Arber, T. D., Culhane, J. L., & Acton, L. W. 1998, Nat, 393, 545
Sams, B. J., Golub, L., & Weiss, N. O. 1992, ApJ, 399, 313
Schrijver, C. J. et al. 1999, Solar Phys., 187, 261
Sobotka, M., Brandt, P. N., & Simon, G. W. 1997, A&A, 328, 689
Stanchfield, D. C. H., Thomas, J. H., & Lites, B. W. 1997, ApJ, 477, 485
Title, A. M., Frank, Z. A., Shine, R. A., Tarbell, T. D., Topka, K. P., Scharmer, G., & Schmidt, W. 1993, ApJ, 403, 780
Vaiana, G. S., Zombeck, M., Krieger, A. S., & Timothy, A. F. 1976, Ap&SS, 39, 75
Vourlidas, A., Bastian, T. S., & Aschwanden, M. J. 1997, ApJ, 489, 403
Westendorp Plaza, C., del Toro Iniesta, J. C., Ruiz Cobo, B., Pillet, V. M., Lites, B. W., & Skumanich, A. 2001, ApJ, 547, 1130
Winebarger, A. R., Warren, H. P., & Mariska, J. T. 2003, ApJ, 587, 439